RESEARCH TRIANGLE INSTITUTE

Fifth Quarterly Progress Report

September 26 through December 26, 1984

NIH Contract NO1-NS-2356

Speech Processors for Auditory Prostheses

Prepared by

Blake S. Wilson and Charles C. Finley

Neuroscience Program Office
Research Triangle Institute
Research Triangle Park, NC 27709

CONTENTS

I. Introduction

The purpose of this project is to design and evaluate speech processors for multichannel auditory prostheses. Ideally, the processors will extract (or preserve) from speech those parameters that are essential for intelligibility and then appropriately encode these parameters for electrical stimulation of the auditory nerve on a sector-by-sector basis. Initial efforts have been directed at the development of a variety of tools to aid in the design of the speech processors. The most important of these tools are (a) a computer-based simulator for rapid and practical implementation of many processors in tests with single subjects and (b) an integrated field-neuron model for understanding (and later controlling) the events of intracochlear electrical stimulation. At present, all major development efforts are completed or essentially completed, and our focus now is on application of these powerful tools. For example, insights into the physical mechanisms of intracochlear electrical stimulation, derived from application of the integrated field-neuron model, have lead us to formulate new strategies for coding speech with auditory prostheses. The emphasis of our work in the immediate future will be on the evaluation of these strategies in tests with experimental subjects both at the University of California at San Francisco (UCSF) and at the Duke University Medical Center. Work in the present quarter included the following:

1. Participation in the 15th Annual Neural Prosthesis Workshop last November;

2. Preparation and presentation of material for a site visit at RTI by Drs. Hambrecht and Loeb of the NIH;

3. Participation as collaborating members of the UCSF team for a NIH site visit in San Francisco on January 15;

4. Installation and checkout at UCSF of the hardware interface for communication between the Eclipse computer and implanted electrodes, with identification of several remaining problems to resolve;

5. Installation and checkout at UCSF of the software for the computer-based simulator of speech processors for auditory prostheses;

6. Further development and application of the integrated field-neuron model, including (a) modifications to allow calculation of field potentials in the plane of the UCSF electrode array spiral and (b) an initial examination of the effects of bone-fluid interfaces on current densities in the scala tympani and in excitable tissue;

7. Further development and refinement of the computer-based simulator, including the addition of (a) various signal-processing modules, (b) improved user-interface code, (c) improved graphics support, and (d) software patches to allow access to the Interactive Laboratory System (ILS) modules available at UCSF; and

8. Preparation for the first implant patient at Duke, including (a) coordination of parallel efforts at UCSF and Storz Instrument Company in St. Louis, (b) construction of a laboratory at Duke that is functionally identical to the laboratory we have helped to construct at UCSF for evaluation of cochlear-implant patients, and (c) review of prospective implant patients.

In addition to the work just outlined, we are pleased to note the addition of two new members to our staff: Dewey Lawson, Ph.D., a physicist with extensive background in computer science and speech analysis, and Kathrinn Fitzpatrick, who will act as a part-time secretary and administrative assistant for our group.

In this report we will describe in detail our further work on the integrated field-neuron model (point 6 above). Discussion of the efforts indicated in points 7 and 8 is deferred for now, but will appear in future quarterly reports.

II. Further Development and Application of the Integrated Field-Neuron Model

Our general approach to the design of speech processors for auditory prostheses is based in large part on the recognition that the most-critical function of the prosthetic system is to exert control over the patterns of single-unit discharge in the auditory nerve. Consequently, we have placed emphasis upon defining the characteristics of the "electrical-to-neural transformer" in the implanted ear, which govern and limit our ability to achieve desired firing patterns. The integrated field-neuron model is a major tool being developed to help define these characteristics. The following subsections describe two areas in which the field-neuron model has been advanced in the past quarter.

Field patterns in the two-dimensional plane containing the UCSF electrode spiral

The integrated field-neuron model has been expanded to include calculations of field patterns in the plane of the electrode array spiral. Calculations in this plane provide an estimate of field patterns over the entire extent of the electrode array, as opposed to the local field patterns of the cross-sectional calculations described in Quarterly Report 2. Figure 1 shows the position of each of the sixteen electrodes of the UCSF electrode array when viewed from above the plane of the electrode array spiral. Positions are determined both by the electrode placement in the silastic carrier and by the spiral configuration of the array itself, the latter of which is determined by the assembly's mechanical memory. Each electrode is indicated by the closed circles, and the center line of the silastic carrier is shown by the spiral curve. Perpendicular to the spiral are short lines indicating the positions of radially-directed dendrites, spaced at one millimeter intervals along the spiral. Potential field patterns are calculated using the finite-difference method described in previous quarterly reports. The tissue medium for calculations in the plane of the spiral is assumed to be homogeneous and therefore the results do not reflect possible effects of impedance differences at tissue boundaries. Evaluation of this assumption of uniform tissue properties is addressed later in this

UCSF ELECTRODE ARRAY

showing spiral of mechanical memory,
positions of 16 electrodes, and
locations of 20 radial dendrites spaced at
1 mm. intervals along the spiral.

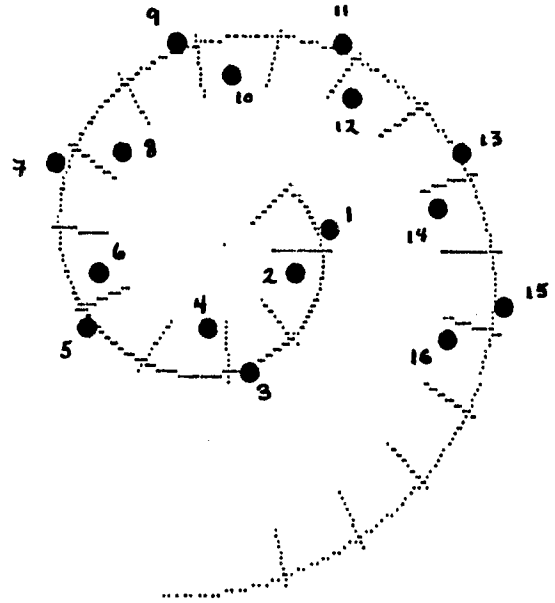

FIGURE 1

report.

Figure 2 illustrates the results of a field calculation with the two most-apical electrodes energized. Electrode [1] is polarized with a positive voltage and electrode [2] is polarized with a negative voltage of equal magnitude. Computations are conducted with the outer boundary held to zero. The right panel shows isopotential contours in a subsection of the plane. Also shown are the electrode locations and spiral path of the electrode array. The locations of radial dendrites are labeled A-T, with an arrowhead pointing to the modiolar (or most medial) end of each dendrite. The left side of Figure 2 indicates the potential levels along the locus of each dendrite, A-T. The ordinate of each small panel is voltage, ranging from the positive voltage magnitude at the most apical electrode [1] to the negative voltage magnitude at the next adjacent electrode [2]. The abcissae indicate positions along the dendrites.

Evaluation of the resultant potential profiles suggests that the fields in the vicinity of the apical stimulating pair are highly asymmetrical and also could stimulate a portion of the adjacent, more basal turn of the cochlea. To illustrate, dendrites D, E, L and M lie close to the 50% isopotential contour. Panels D, E, L and M show essentially zero stimulus voltage along the length of these dendrites. Therfore, these neural elements would be little affected by stimuli delivered to electrodes [1] and [2]. In contrast, dendrites H and Q are located at opposite poles of the bipolar stimulus field and consequently have significant and nearly-constant voltages imposed along their lengths. Responses of neurons at these locations could produce "turn-to-turn crosstalk" in percepts elicited by relatively-intense stimuli. Finally, as expected, the greatest potentials appear in the immediate vicinity of the electrodes. Dendrite S, which is located midway between the offset bipolar pair, has a steep gradient from positive to negative along its length. Dendrites R and T, which are equidistant from the electrode pair along the basilar membrane, have less steep gradients and only one polarity of imposed potentials. If the magnitude of the imposed potentials along the dendrite is the excitatory aspect of the stimulus (as opposed to the voltage gradient along the dendrite or some combination of gradient and magnitude), as has been suggested by our applications of the Frankenhauser-Huxley model of frog axons (see Quarterly Report 4) and by the work of others with models of mammalian myelinated nerve (see, e.g., Ranck, 1975), dendrite R will have a

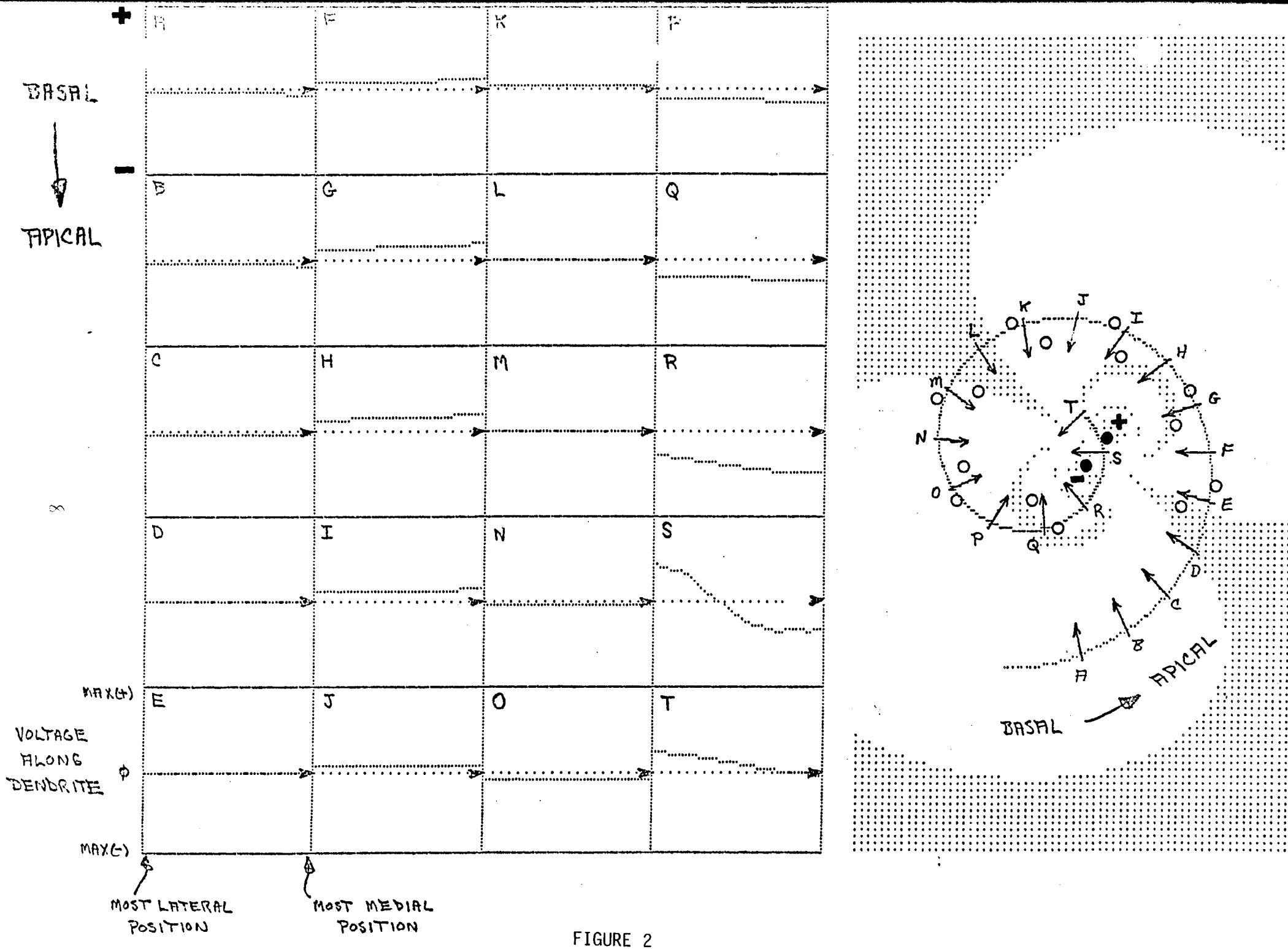
BASAL
APICAL
A
F
K
P
B
G
L
Q
C
H
M
R
D
I
N
S
E
J
O
T
MAX(+)
VOLTAGE ALONG DENDRITE
Φ
MAX(-)
MOST LATERAL POSITION
MOST MEDIAL POSITION
BASAL
APICAL

FIGURE 2

threshold of response that is 2 or 3 times lower than the threshold of response for dendrite T. This difference of stimulus magnitudes is notable for these equidistant positions, indicating a significant asymmetry in the effective field of stimululation for the bipolar pair. This asymmetry is largely due to the curling of the cochlear spiral into one of the poles of the bipolar electrode pair.

It should be noted that the above situation would most likely correspond to that of a patient in whom dendrite survival is good. The continued medial course of the neurons through the cochlea and into the modiolus is not depicted here. Modeling of this more complex situation must await expansion of the model to three dimensions.

Figure 3 provides a high-resolution picture of voltage profiles produced along dendrites in the implanted ear for the stimulus conditions of Figure 2. In Figure 3, a continuum of dendrite positions is presented from the most-basal to the most-apical positions of the electrode array. The three panels show the extracellular stimulus voltage at the most-medial, the mid, and the most-lateral positions of the dendrites. The abcissae indicate positions along the basilar membrane from basal to apical. The midpoint positions of each bipolar pair are indicated by the vertical lines, with the relative position of each electrode indicated by its number. Midpoint positions of bipolar electrode pairs are 2 mm. apart along the basilar partition.

Figure 4 shows the same potential distribution information as Figure 3, except the potential distributions are shown for the condition of electrode [3] being positive and electrode [4] being negative. The distributions shown in Figures 3 and 4 are essentially equivalent with minor amplitude differences appearing in the medial and midpoint dendrite positions. These differences arise because of the more medial placement of electrode [4] relative to the spiral centerline than for electrode [2]. This is due to the tapering of the silastic carrier at the electrode array tip.

An additional detail seen in Figure 4 is the double line shown in the upper portion of the top panel. This line depicts an approximation of the "effective stimulus field" of the electrode pair, driven with a balanced biphasic pulse. The effective stimulus field is best interpreted as a profile of the probabilities of firing for the neuronal pool that is affected by the stimulus. This profile is derived by plotting the peak, absolute values of the potential levels at the medial, midpoint and lateral

OFFSET BIPOLAR
CONFIGURATION
(1-2)

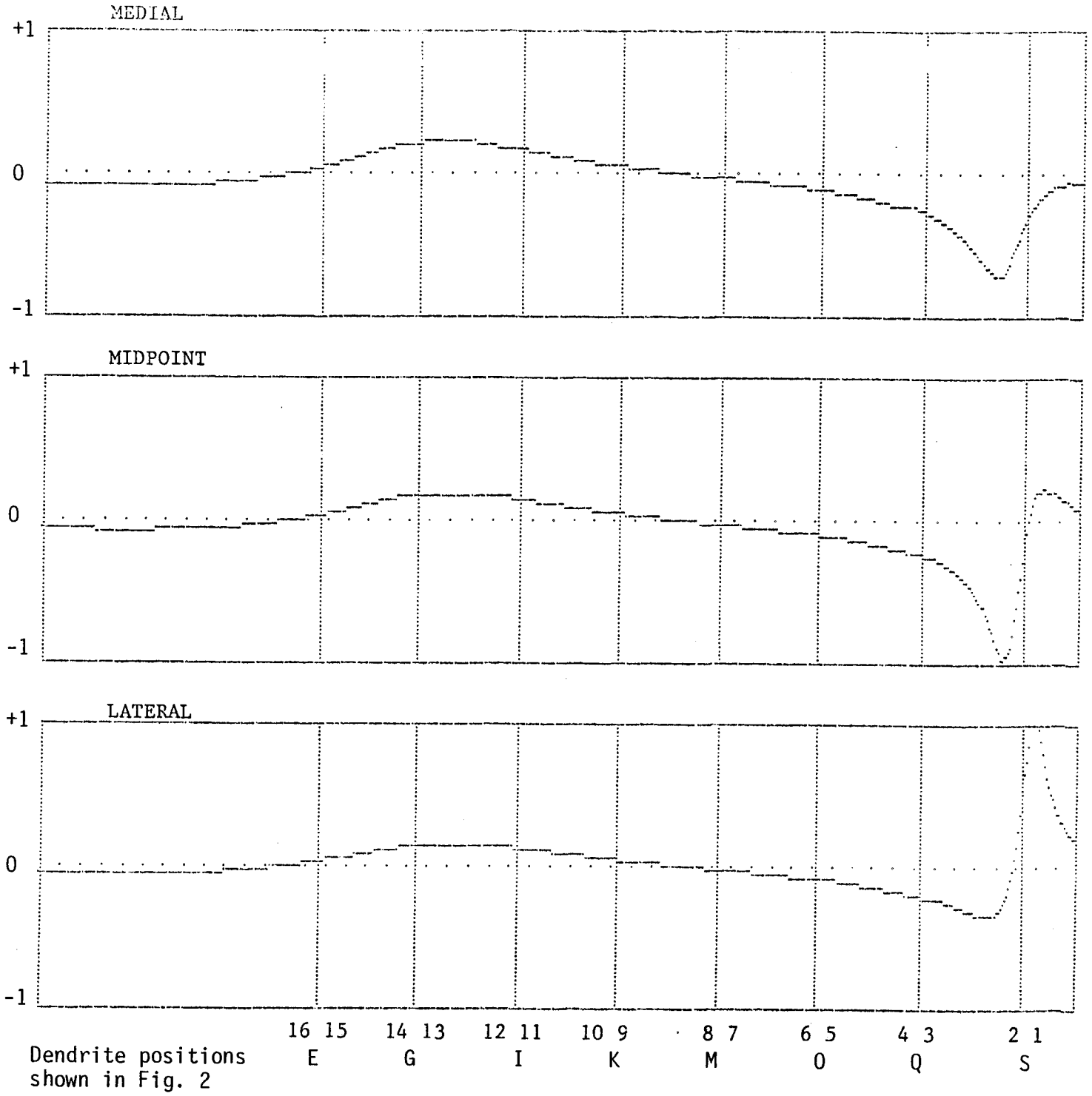

FIGURE 3

OFFSET BIPOLAR

CONFIGURATION

(3-4)

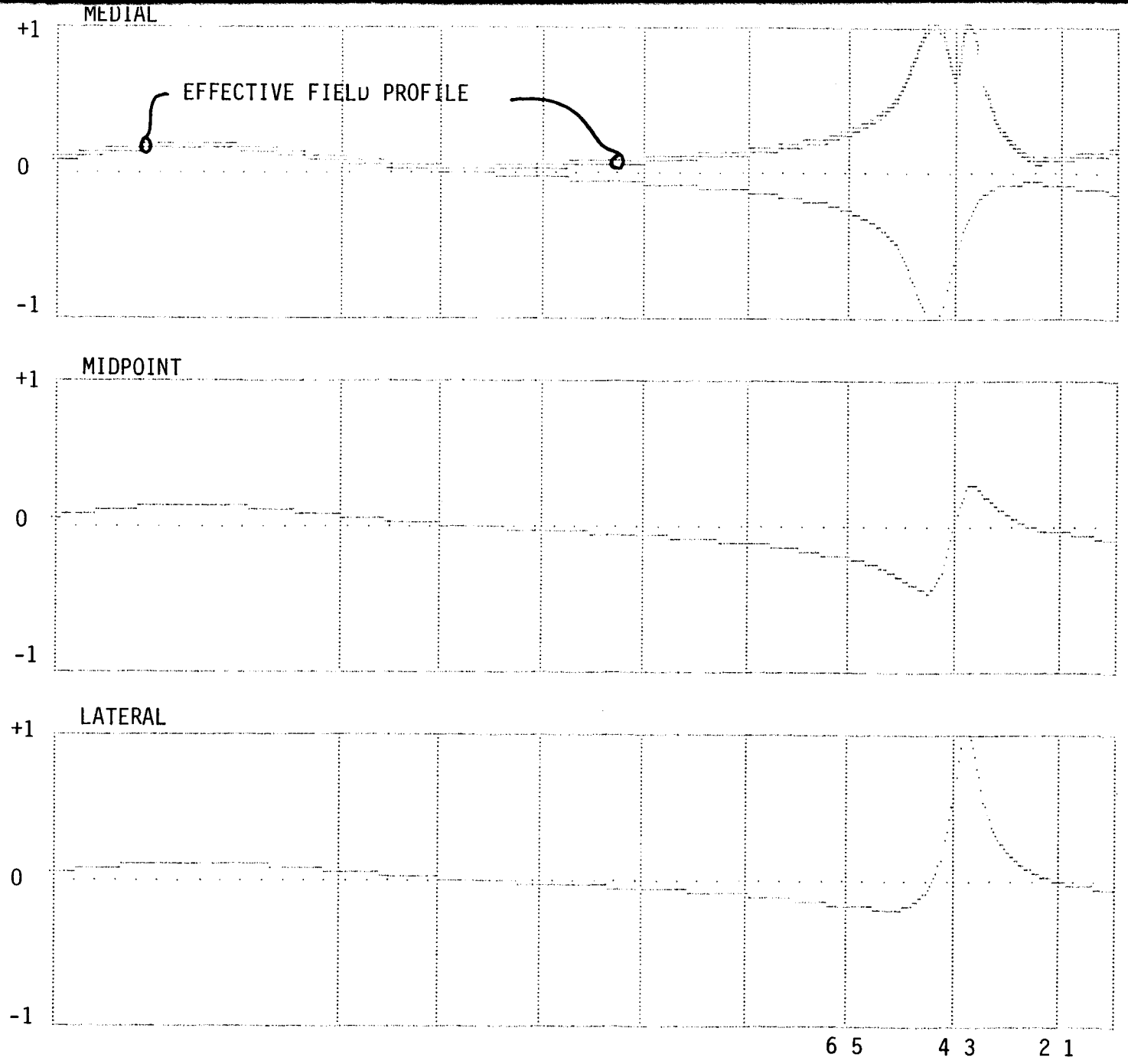

FIGURE 4

dendrite positions, which roughly correspond to node locations along the dendrites. Absolute values are used to account for the effects of both phases of the balanced biphasic pulse. Peak values are used since the most strongly driven node along the dendrite will have the highest probability of firing. The representation thus obtained is a first approximation of the firing probabilities of neurons along the basilar partition in response to a balanced biphasic stimulus applied across a bipolar electrode pair. Temporal features of the stimulus and the neural response are neglected, and consideration of anatomical variations (e.g., fiber diameters) is not made. Tissue impedance effects have also not been rigorously modeled (see later discussion). Despite these inherent limitations of the present model, it is instructive to examine the derived effective stimulus fields of both single- and multiple-channel stimulation.

The effective stimulus field shown in Figure 4 has a complex, double peaked profile with asymmetrical roll-off rates beyond the peaks. The double peaking is due to the offset configuration of each of the dipole pairs of the UCSF array. This follows intuitively if one considers that each electrode will have its own sphere of maximal influence in the region nearest the electrode and that the electrodes are physically displaced along the basilar partition. The asymmetrical roll-offs are largely due to the spiral shape of the electrode array which curls toward or away from the axis of the stimulating electrode pair. An interesting point that arises here is that substantial sharpening (narrowing) of the effective stimulus field of an offset dipole pair might be obtained by using an asymmetrical biphasic pulse, as compared to the effective stimulus field that occurs with a symmetrical biphasic pulse (i.e., one of the two peaks of the effective stimulus field could be "selected" with the use of asymmetrical biphasic pulses). A possible test of this hypothesis is to determine if a patient with good dendrite survival can distinguish between an asymmetrical, balanced biphasic stimulus and a similar stimulus, but of opposite polarity, applied to the same electrode pair. In such a patient, different populations of fibers (with some overlap) would be excited with each stimulus, and the resulting percepts should be distinguishable if our model of stimulus profiles is essentially correct.

Similar examination is instructive for the case of simultaneous stimulation of adjacent dipole pairs. This stimulus condition often results in considerable channel interactions in which stimulus fields for the

adjacent dipoles appear to overlap. For the present discussion, only the situation of simultaneous stimulation with symmetrical biphasic pulses is considered. Figure 5 shows the potential profiles when both dipole pairs are stimulated simultaneously. This is equivalent to summation of the data shown previously in Figures 3 and 4. Note that the ordinate range in Figure 5 is twice the range shown in Figures 3 and 4. The effective stimulus field for the combined stimulation is also shown in Figure 5 as the double line. Figure 6 shows the opposite situation in which the stimulus polarity of the biphasic pulse applied to electrodes [1] and [2] has been reversed. Again, the effective stimulus field is indicated by the double line. One point to note is that the effective stimulus fields in Figure 5 and 6 are identical. This result is a simple consequence of superposition of the stimuli, and is consistent with the results of channel-interaction experiments conducted with patients in whom dendrite survival appeared (by several measures) to be good. That is, for the good-survival case one would expect the threshold of responses to in-phase stimuli delivered to the two electrode pairs to closely approximate the threshold of responses to out-of-phase stimuli. This expectation is, in fact, borne out in the experimental results for such patients. However, for the case of poor or patchy survival of dendrites, the effective stimulus field will no longer correspond to that plotted in Figures 5 and 6 because the absence of stimulable neural elements at certain locations will skew the population of responding neurons. This skew would manifest itself in the form of significant channel interactions and significant differences in the thresholds to in-phase and out-of-phase stimuli. These predictions are entirely consistent with the results of channel-interaction experiments conducted with patients in whom dendrite survival appeared to be poor. Therefore, channel interactions and related phenomena are the likely result of uneven survival of dendrites, as opposed to the currently-held notion of significant overlap in the stimulation fields.

Although the results presented above have clear significance for the design of speech processors for auditory prostheses, it is important to remember that several assumptions underlie the model in its present, simplified form. The major assumption of the spiral-plane model is that the characteristics of tissue in the plane of computation are homogeneous. An obvious method for evaluating this and other assumptions in the model is to compare model predictions with the results of animal experiments in which

OFFSET BIPOLAR

CONFIGURATION

(3-4)

plus

(1-2)

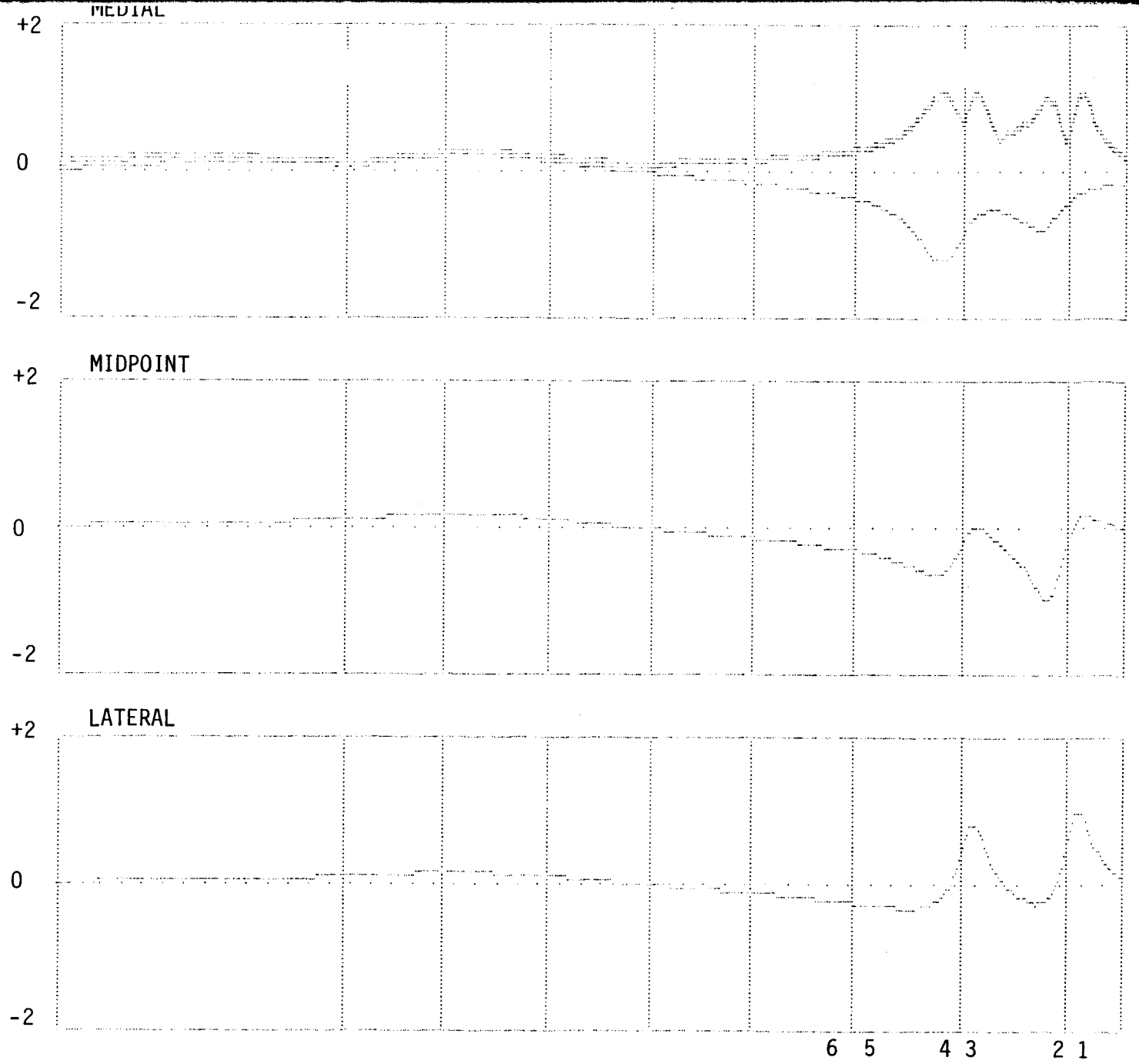

FIGURE 5

OFFSET BIPOLAR

CONFIGURATION

(3-4)

minus

(1-2)

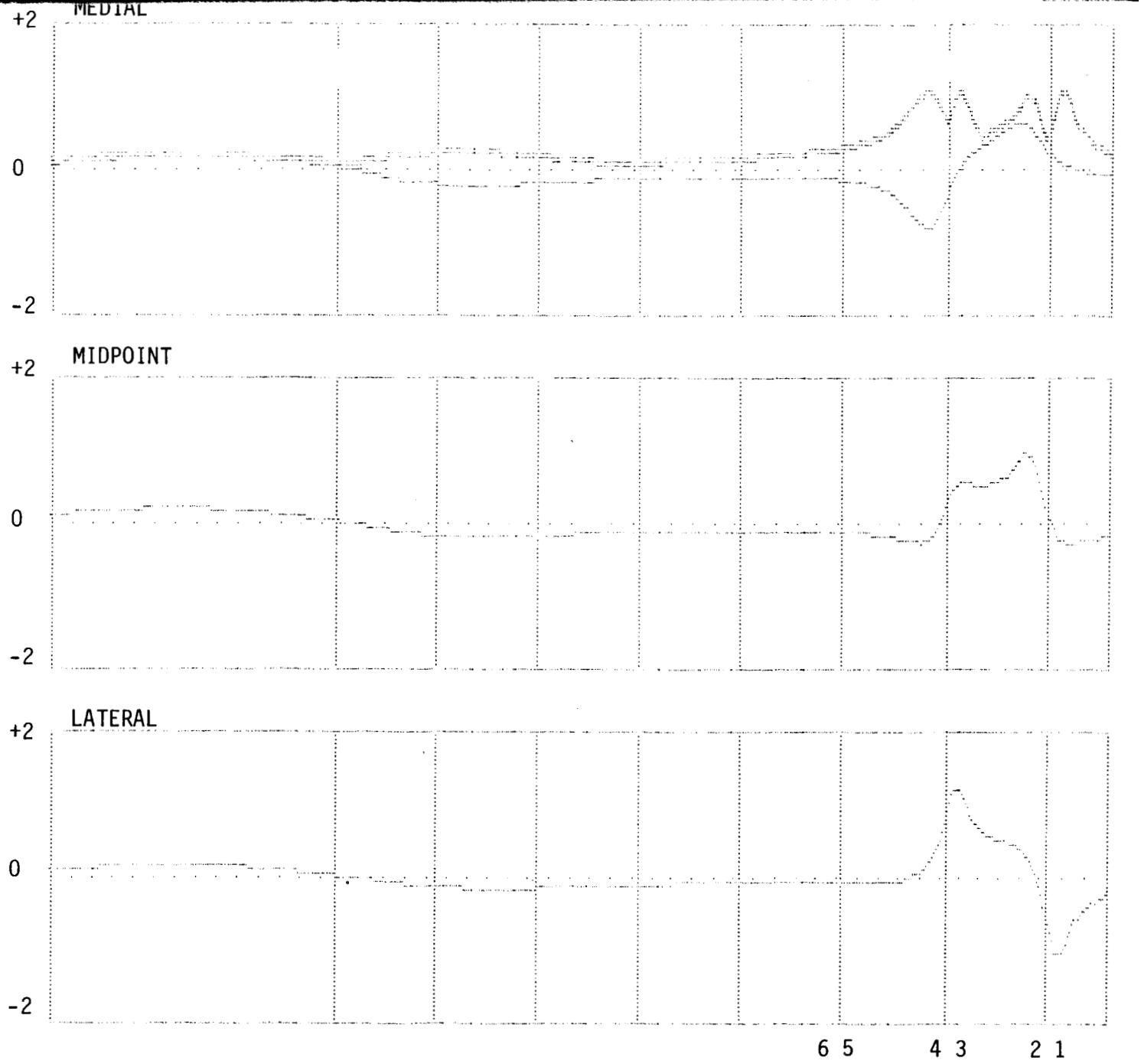

FIGURE 6

direct measurements of stimulus-response fields can be made. One such set of experiments was performed at UCSF in the late 70's with an array of aligned bipolar electrodes placed in the scala tympani of adult cats (see, e.g., Merzenich and White, 1977). Figure 7 shows an aligned UCSF electrode array on the scale of the human implant. Each electrode of each dipole pair is located on the same radial line. This configuration has not been used in patients but, as just mentioned, has been used extensively in cat experiments. Figure 8 shows the potential distributions calculated by the model for the aligned array of Figure 7 with electrodes [3] and [4] being driven. The effective stimulus field is derived as described above, and is displayed in the top panel. Superimposed on the effective stimulus field is the curve of exponential falloff in the response fields measured for "well-positioned" electrodes in the cat (space constant = .87 mm.; see Merzenich and White for details). The match of the data from the model and experimental results is truly remarkable, suggesting that the present approach to modeling is justified at this level of analysis. However, additional comparisons must be made to verify the model's accuracy for other situations and, more generally, direct evaluation of the assumptions in the model should be made before we accept its predictions as valid. A direct evaluation of tissue-impedance effects (and the related assumption of uniform tissue properties) is therefore presented in the following subsection.

Initial studies on the effects of tissue impedances and the path of current flow with bipolar stimulation by the UCSF electrode array

Figure 9 shows two depictions of the aligned UCSF electrode array in cross-section. Refer to Quarterly Report 2 for a more complete description of the computations involved in the cross-sectional model. A concentric ring which surrounds the silastic insulator and electrodes has been added to the model. This ring mimics the interface between the perilymph, which surrounds the electrode array in the scala tympani, and the bony wall of scala tympani. In the figure on the left, tissue characteristics have been set such that bone begins immediately at the surface of the silastic carrier and the electrodes. This condition mimics the condition assumed for all model calculations reported in the previous quarterly reports. On the right

ALIGNED BIPOLAR

UCSF CONFIGURATION

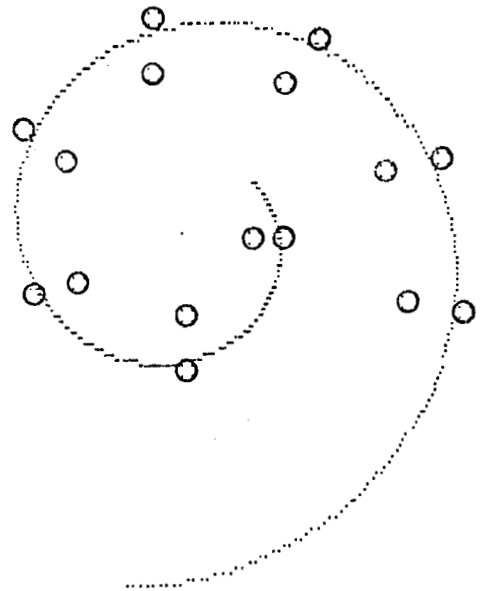

FIGURE 7

ALIGNED BIPOLAR

CONFIGURATION

(3-4)

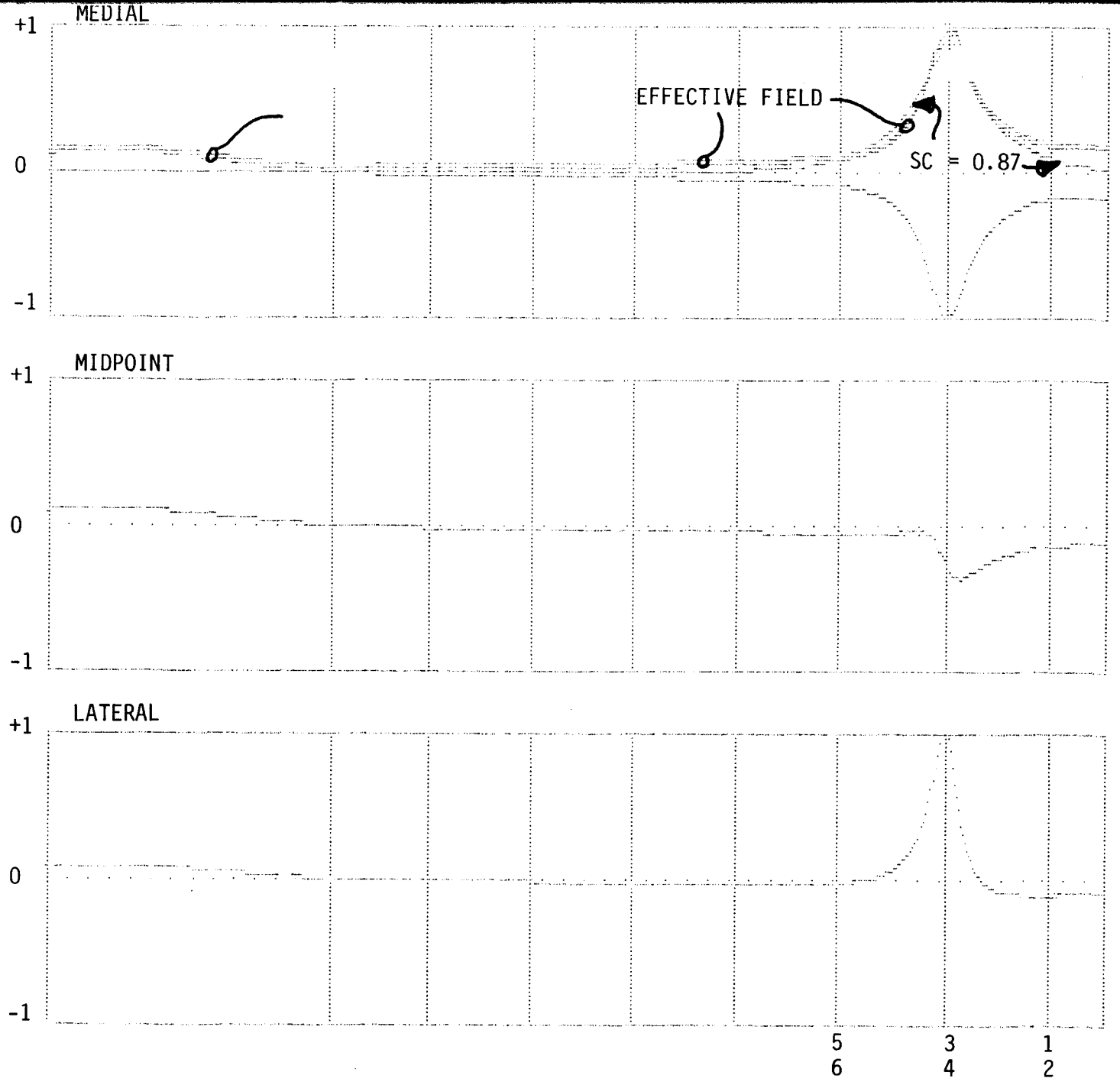

FIGURE 8

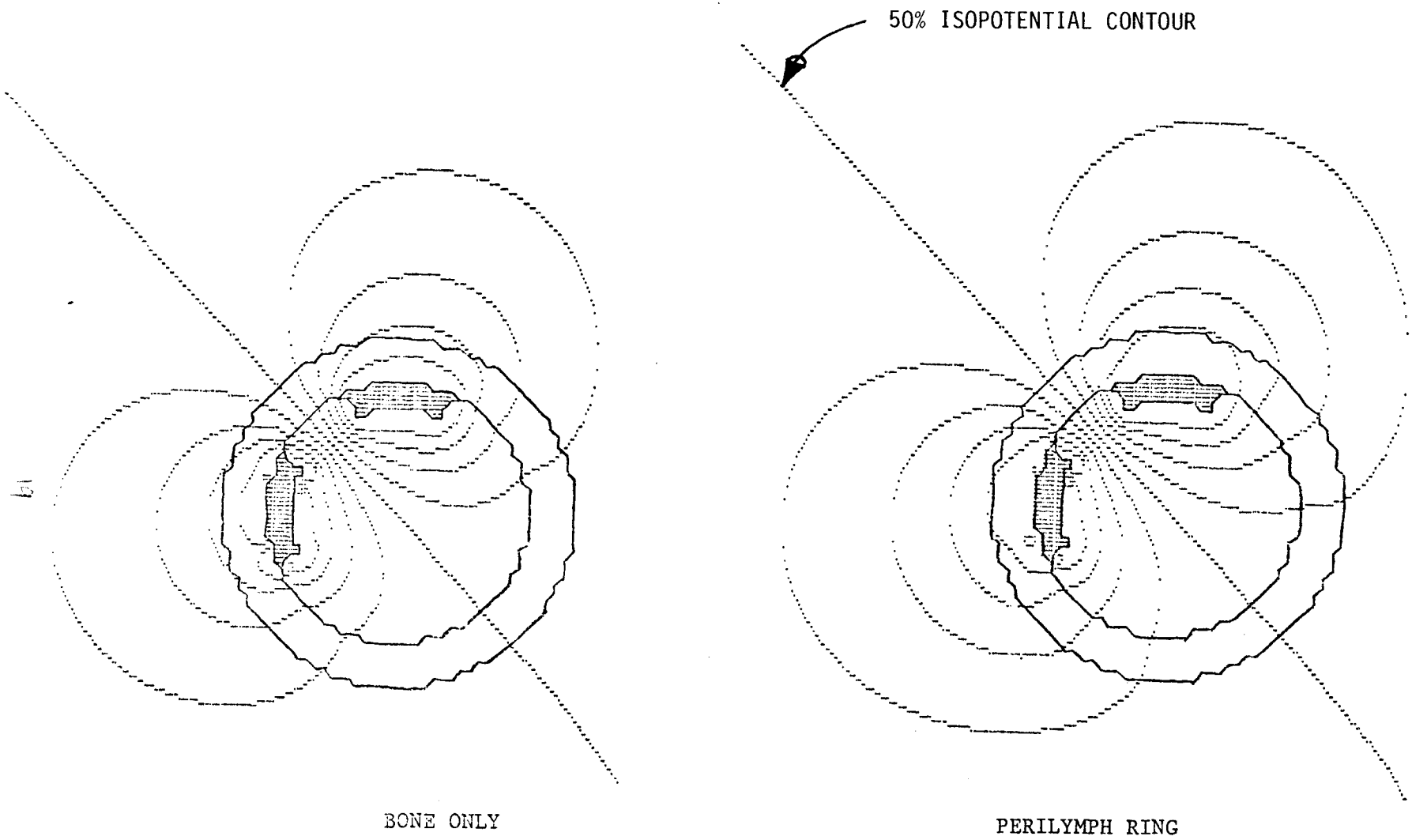

10 % ISOPOTENTIAL CONTOURS FOR ALIGNED UCSF BIPOLAR ELECTRODES

Resistivities:
Insulator - 10^7 ohm-cm
Bone - 800 ohm-cm
Perilymph - 300 ohm-cm

FIGURE 9

is the same computation, but with the perilymph ring retaining true perilymph characteristics. A slight expansion of the isopotential contours can be observed when the perilymph ring is included.

Figure 10 shows lines of constant magnitude of current flux for the same two conditions described above for Figure 9. Isocurrent contours are shown at 5% intervals between the peak current flux flowing between the electrodes and zero. Note that with the perilymph ring included the isocurrent contours are more tightly constrained and do not spread significantly into the bony tissue. It is important to observe here, however, that the relative impact between the two conditions is relatively minor. At best, only about 10 % of the total current flux flows out to where the bony interface would lie in either set of conditions. In fact, the bulk of current flows immediately along the surface of the silastic insulator between the two electrodes.

Figure 11 gives a better perspective of the pattern of curent flow between the electrodes. Figure 11 shows the current flux (normalized to the peak flux value) that flows normal to the 50% isopotential contour which lies midway between the two electrodes. Current flux is shown for both bone-only and perilymph-ring conditions. As can be seen, the magnitude of current flux drops rapidly as a function of the distance from the silastic carrier. Little current flows on the back side of the silastic carrier away from the electrodes. The present model assumes a 100 micron wide perilymph ring. In the practical application of the electrode, placement of the electrodes within 100 microns of the bony wall would be extremely good placement with much greater distances expected normally. This would clearly be the case with electrode arrays other than the UCSF array, which do not have mechanical memories. Consequently, it is expected that relatively-small amounts of the injected stimulation current actually pass through the bony tissues. Rather, most of the current is shunted through the perilymph. In this case, we believe that simple modeling of the tissue impedances as being homogenous is a reasonable, first approximation to make.

One point to emphasize, however, is that this approximation is probably only valid in the case of bipolar stimulation. In the instance of monopolar stimulation to a remote reference, the bulk of the current flux leaving the electrode must necessarily flow across tissue boundaries. In this case, we believe that tissue impedances will play a substantial role in the behavior of the system. Further refinement of the present model will be required to

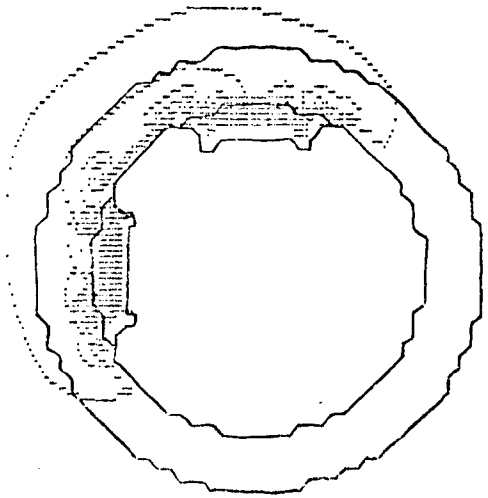

BONE ONLY

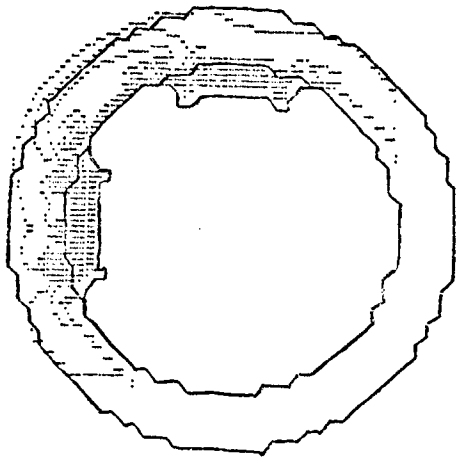

PERILYMPH RING

5 % Constant Magnitude Current Flux Lines

FIGURE 10

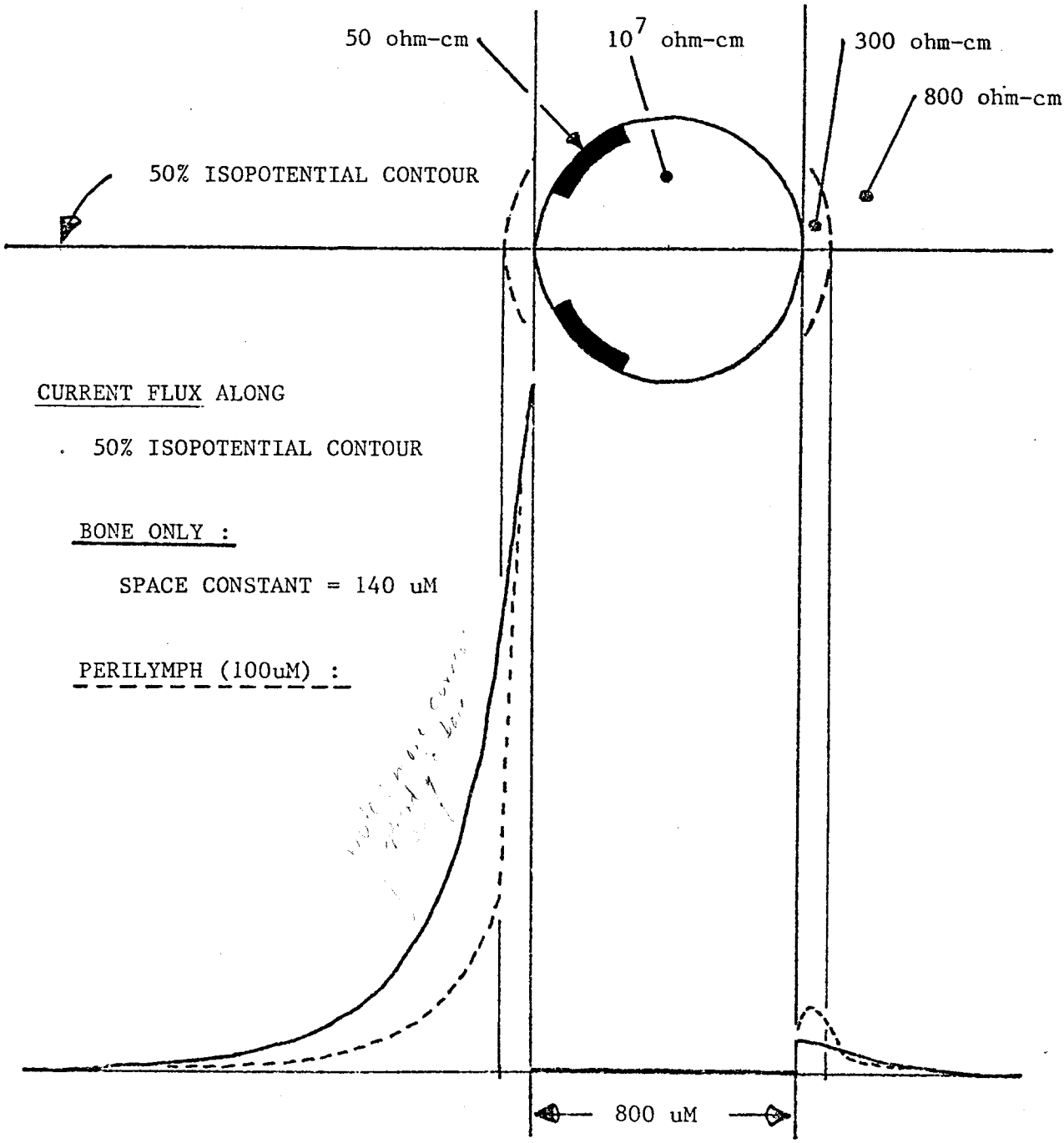
50 ohm-cm
10^7 ohm-cm
300 ohm-cm
800 ohm-cm
50% ISOPOTENTIAL CONTOUR
CURRENT FLUX ALONG
50% ISOPOTENTIAL CONTOUR
BONE ONLY :
SPACE CONSTANT = 140 uM
PERILYMPH (100uM) :
800 uM

FIGURE 11

accurately describe monopolar stimulation.

III. Plans for the Next Quarter

As usual, we expect the upcoming quarter to be a busy one. The most-important activity of the quarter will be to prepare for tests with implant patients both at UCSF and Duke. The tests at UCSF will be conducted in the last week of February and will include studies (a) to confirm that computer-based simulation of the present, analog UCSF speech processor produces results essentially identical to those obtained with the UCSF processor and (b) to evaluate several alternatives to the present UCSF processor for coding speech with four-channel auditory prostheses. Because the patient who will participate in these studies is fitted with the four-channel transcutaneous system for transmission of information to the electrode array, we will not be able to conduct experiments that either require percutaneous access to the electrodes or more than four channels of stimulation. Inasmuch as most of our planned experiments fall into this latter class, our studies with this patient will be relatively limited and brief. The UCSF team has identified three candidates for participation in the next experimental series at UCSF, which is expected to begin in late May or early June. All patients in this series will have percutaneous cables and will be intensively studied by the UCSF/RTI team.

In the meantime, we expect to implant a patient at Duke in late March. Fourteen candidates have been identified for possible implant operations, and four of these people may qualify as participants in an experimental series. The first and subsequent patients at Duke will be fitted with a percutaneous cable so that we can conduct our full range of evaluations.

To prepare for the upcoming tests at Duke, we now have under construction a laboratory that is functionally identical to the laboratory we have helped to construct at UCSF for evaluation of cochlear-implant patients. The laboratory at Duke will include an Eclipse computer system and another hardware interface for communication between the Eclipse and implanted electrodes. All costs for this laboratory will be covered by sources other than the present contract. We expect to have the laboratory completed before April, in time for tests with the first patient at Duke.

Additional activities of next quarter will include (a) presentation of two papers at the ARO meeting this February; (b) conduct of animal experiments in collaboration with Dr. M. M. Merzenich and others at UCSF, to confirm various predictions of the integrated field-neuron model and to

evaluate our strategies for measuring and interpreting intracochlear evoked potentials; and (c) installation of the neural component of the integrated field-neuron model on the AD-10 differential-equation processor of the National Biomedical Simulation Resource (NBSR) at Duke. Although we had planned activity (c) for the previous quarter of project work, legal difficulties arising from software licensing agreements delayed our access to the NBSR equipment. These difficulties have now been resolved, however, and we expect to have our integrated field-neuron model running at the NBSR in mid March.

IV. References

Ranck, J. B., Jr. 1975. Which elements are excited in electrical stimulation of mammalian central nervous system? Brain Res. 98: 417-440.

Merzenich, M. M. and White, M. W. 1977. Cochlear implant -- The interface problem. In F. T. Hambrecht and J. B. Reswick (Eds.), Functional Electrical Stimulation: Applications in Neural Prostheses, Marcel Dekker, Inc., pp 321-340.